Anomalous Hall effect related to the magnetization in pure decagonal Al-Mn phases

A. Gozlan, C. Berger, and G. Fourcaudot
Laboratoire d'Etudes des Propriétés Electroniques des Solides,-CNRS, Boîte Postale 166, 38042 Grenoble CEDEX, France

R. Omari, J. C. Lasjaunias, and J. J. Préjean
Centre de Recherches sur les Très Basses Températures,-CNRS, Boîte Postale 166, 38042 Grenoble CEDEX, France
(Received 22 January 1991)

An anomalous Hall effect is measured in pure decagonal $Al_{80}Mn_{20}$ and $Al_{78}Mn_{22}$. We show that the Hall resistivity ρ_H is linear with the magnetization M measured for the same fields and temperatures: $\rho_H(H,T)=R_0H+4\pi R_S M(H,T)$. The very dominant term $R_S M$ of ρ_H reveals a strong spin-orbit scattering, which is observed in Al-Mn quasicrystals. R_S is found to be temperature independent in the range 6.5–110 K. From our susceptibility, specific-heat, and magnetoresistance data, we deduce that M results from a very low fraction of magnetic moments, which increase drastically with the nominal Mn concentration and that are correlated by Ruderman-Kittel-Kasuya-Yosida interactions. In this respect, the Al-Mn decagonal phase behaves very similarly to previously measured Al-Mn icosahedral and amorphous phases.

INTRODUCTION

Among all the quasicrystals (QC's) discovered so far and characterized by fivefold, eightfold, tenfold, and twelvefold rotation symmetries, the decagonal (T) phase[1] is of particular interest. Indeed, contrary to the icosahedral (i) phase,[2] which is a three-dimensional QC, it possesses one axis of periodicity perpendicular to the quasiperiodic planes. This phase is therefore often presented as an intermediate state between icosahedral and crystalline phases and may be of particular importance in the search for specific behavior due to quasiperiodicity.

From the structural view point the T and i phases seem to be closely related, and their orientational relationships were observed by transmission electron microscopy[3] and by x-ray or neutron diffraction where the intensities are also correlated.[4] Extended x-ray-absorption fine structure (EXAFS) measurements[5] also indicate that somehow similar environments exist in T- and i-Al-Mn alloys and in the cubic α-$Al_9Mn_2Si_2$ phase. This supports structural models using Mackay's icosahedra as the basic structural unit that might be slightly distorted in the T phase.[5] On the other hand, the structural anisotropy of the decagonal phase is outlined in models consisting of a periodic stacking of two-dimensional quasilattices, for instance with two kinds of layers derived from the Penrose pattern.[6]

Besides the recently discovered stable Al-Cu-Co and Al-Co-Ni T phases,[7] which allow us to investigate directly the effect of structural anisotropy on single grains,[8] a comparison between pure amorphous (a), i, T, or crystalline phases in the same system and at similar concentration may be helpful in the investigation of structural and physical properties. Such a comparison is available in the Al-Mn:Si system for which these different structures can be obtained as single phases around 20 at. % Mn. Previous studies[9–11] were devoted to the physical properties of the i, a, and crystalline Al-Mn:Si phases; for instance, the i and a phases present a weakly magnetic behavior (as observed by magnetoresistance, magnetic susceptibility, and specific heat) that increases sharply with the nominal Mn concentration in the sample. In particular i-$Al_{73}Mn_{21}Si_6$ was shown[12] to contain only a low fraction of magnetic moments that order in a spin-glass state at low temperature. On the other hand, the corresponding crystalline phases o-$Al_{86}Mn_{14}$, β-Al_9Mn_3Si, and α-$Al_9Mn_2Si_2$ present no local magnetic moments. In this context, the study of the physical properties of a two-dimensional (2D) Al-Mn quasicrystal having one axis of periodicity is of particular interest, but only a few papers up to now have been published on this subject.[13,14]

We present here low-temperature transport (resistivity, magnetoresistance, and Hall effect) and magnetic properties (susceptibility, magnetization, and specific heat) on pure melt-spun T-$Al_{80}Mn_{20}$ and T-$Al_{78}Mn_{22}$ phases. From the analysis of the χ_{ac} and C_P data, we deduce the presence of a low fraction of magnetic moments that increase with the Mn concentration in the sample (Sec. III) and interact through Ruderman-Kittel-Kasuya-Yosida (RKKY) interactions (Sec. IV). These results are similarly found in icosahedral and amorphous phases. We then focus on the first measurement of an anomalous Hall resistivity linear with the magnetization, that reveals a strong spin-orbit scattering (Sec. V). The resistivity results (Sec. VI) are consistent with this analysis.

I. EXPERIMENTAL PROCEDURE

The samples were prepared using a melt-spinning technique under a helium atmosphere. Details of sample

 ©1991 The American Physical Society

preparation and structural characteristics are given elsewhere.[15] The structure of the samples was determined by x-ray diffraction and by transmission electron microscopy. Pure decagonal phase samples are obtained in as-quenched $Al_{78}Mn_{22}$ and, after annealing, in $Al_{80}Mn_{20}$ (15 h at 300 °C), which eliminates the remaining (fcc) Al phase.

Electrical resistance was measured by using the dc four-probe technique in the temperature range 0.3K–300 K and under a magnetic field up to 8 T. The Hall resistivity was measured using a high-resolution ac bridge with in-phase detection; to account for a possible misalignment of the transverse contacts, five probes were used, and the Hall resistivity was deduced from the odd part of the measurement in the positive and the negative field. The geometrical factor was estimated from weight measurements of the sample. Specific-heat measurements were performed on a dilution refrigerator by means of a transient heat-pulse technique (the same as used in Refs. 10 and 11), the temperature varying step by step, for 150-200 mg of the sample. The magnetic susceptibility χ_{ac} has been measured (in zero external field) in an a.c. field of 1 Oe at a frequency of 22 Hz. The magnetization was measured in a d.c. field in a magnetometer with a resolution of 10^{-7} emu.

II. STABILITY AND MICROSTRUCTURE OF DECAGONAL PHASE

As is already well known, the Al-Mn decagonal phase is metastable, but crystallizes at a higher temperature than the *i*-Al-Mn phase of similar composition.[15] For instance, for *T*-$Al_{78}Mn_{22}$, the high-temperature resistivity of Fig. 1 reveals an irreversible phase transition starting around 950 K (heating rate 20 K/min). In an attempt to increase the decagonal grain size and to reduce the density of defects, the *T*-phase samples were annealed in a series of thermal treatments below the crystallization temperature. After heat treatment of the sample, we observe no significant variation either of the width of the x-ray peaks or of the grain size as seen by transmission electron microscopy (0.5 and 0.7 μm for *T*-$Al_{80}Mn_{20}$ and *T*-$Al_{78}Mn_{22}$, respectively, after 5 h at 500 °C). The

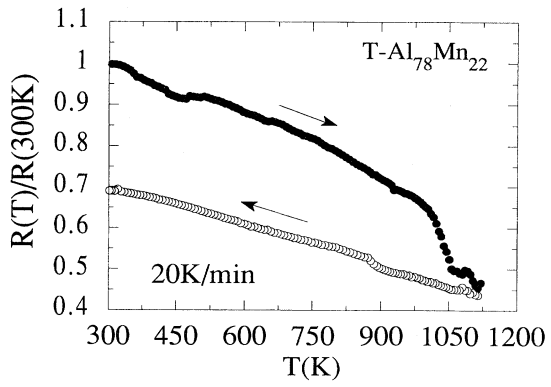

FIG. 1. Reduced electrical resistance $R/R_{300\,K}$ against temperature in decagonal *T*-$Al_{78}Mn_{22}$ at a heating rate of 20 °C/mn. The $R(T)$ curve reveals the irreversible structural transition.

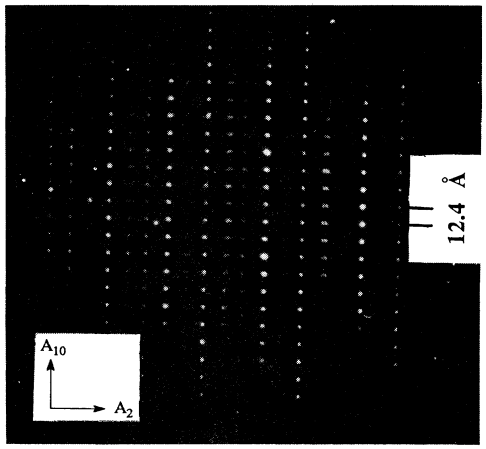

FIG. 2. Electron diffraction pattern taken along a twofold zone axis for decagonal *T*-$Al_{78}Mn_{22}$ phase.

structural anisotropy of this phase is directly observed in the twofold zone axis pattern (Fig. 2): The diffraction spots are periodically spaced along the tenfold axis and give a periodicity of 12.40±0.05 Å for both *T* phases. Along the perpendicular twofold axis, the spots follow a Fibonacci sequence with two length scales 1 and the golden mean τ. However, the study of the microstructure of these samples does not reveal any preferential crystallographic orientation of the individual grains (Fig. 3): Therefore, in the following we cannot directly single out the effect of the structural anisotropy of the *T* phase.

Moreover, both the high resistivity value ($\rho_{0.3\,K}$ = 430±20 and 480±30 $\mu\Omega$ cm for *T*-$Al_{80}Mn_{20}$ and *T*-$Al_{78}Mn_{22}$, respectively) and the temperature dependence of ρ [$(1/\rho)(\Delta\rho/\Delta T) \sim -10^{-4}$ K^{-1} for the two *T*-phases[15]] are very similar to that of an amorphous phase of the same composition *a*-$Al_{78}Mn_{22}$ (Fig. 4). Although the *T* phase is an ordered structure, its resistivity behaves like a disordered alloy that may perhaps be associated to the high density of defects present in the sample.

FIG. 3. Microstructure of decagonal *T*-$Al_{78}Mn_{22}$ phase observed by transmission electron microscopy.

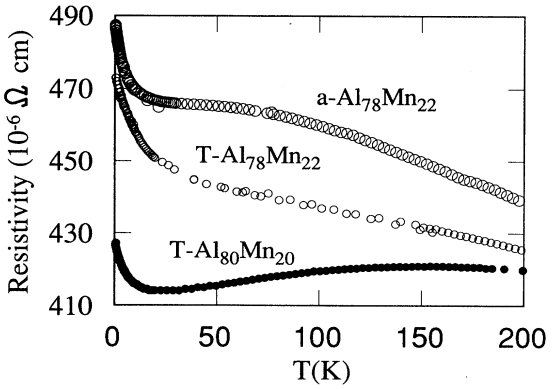

FIG. 4. Temperature dependence of the electrical resistivity for T-$Al_{78}Mn_{22}$ and T-$Al_{80}Mn_{20}$ with a-$Al_{78}Mn_{22}$ for comparison.

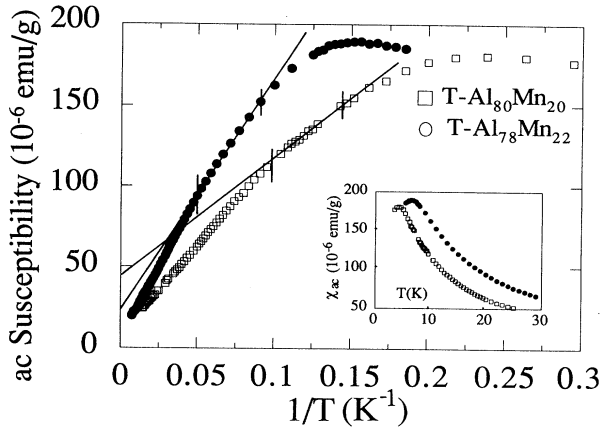

FIG. 5. Susceptibility data χ_{ac} vs $1/T$ for T-$Al_{78}Mn_{22}$ and T-$Al_{80}Mn_{20}$, and the temperature range of the Curie law fit. The inset presents χ_{ac} T for both T phases.

III. EXISTENCE OF MAGNETIC AND NONMAGNETIC Mn ATOMS

Previous studies of i and a Al-Mn phases have suggested the existence of two different classes of Mn atoms, one being magnetic and the other nonmagnetic. For instance, in i-$Al_{73}Mn_{21}Si_6$, the concentration x of the really magnetic Mn's and their moment p_{eff} could be estimated separately by measuring the linear and dc nonlinear susceptibilities:[12] A small concentration of magnetic entities was found ($x=2.7\times10^{-3}$, corresponding to 1.3% of the number of Mn) carrying a high moment value of $7.5\mu_B$. Also NMR studies[16] on Al-Mn QC, and in particular on pure T-$Al_{78}Mn_{22}$, suggest a nonuniform distribution of local magnetism. To obtain the order of magnitude of x in our T phases, we study both the ac susceptibility χ_{ac} and the nuclear hyperfine term C_N provided by specific-heat measurements.

The temperature dependence of χ_{ac} is shown in the insert of Fig. 5. χ_{ac}(22 Hz) exhibits at T_m a maximum of a spin-glass-like type: $T_m=4.2$ K and 6.25 K for T-$Al_{80}Mn_{20}$ and T-$Al_{78}Mn_{22}$, respectively. T_m depends on the frequency ν of the excitation field. But this dependence is very small, as is the case when a true $3d$ spin-glass-transition occurs: T_m(240 Hz) = 6.33 K for T-$Al_{78}Mn_{22}$. To deduce x, we should fit equilibrium susceptibility $\chi_{eq}=\chi_{ac}$ ($\nu=0$) data by a Curie ($\chi=\chi_0+C/T$) or a Curie-Weiss [$\chi=\chi_0+C/(T-\Theta)$] law. For T-$Al_{78}Mn_{22}$, above 11 K = $1.75T_m$, no frequency effects for $\nu\leq240$ Hz are observed within our accuracy ($\Delta\chi/\chi<2.10^{-3}$). Thus χ_{ac}(22 Hz) can be identified with χ_{eq} above 11 K: It is linear in $1/T$ up to 20 K = $3.2T_m$ (see Fig. 5). The same applies for T-$Al_{80}Mn_{20}$ from 7 K up to 12 K. The values of χ_0 and C are reported in Table I. At high temperatures (above $3.2T_m$), deviations to the previous law are observed. They can be due to a small variation of χ_0 at high T and/or to the necessity to introduce a Curie-Weiss temperature: $\chi=\chi_0+C/(T-\Theta)$ as is discussed later on. Below $1.7T_m$, χ_{ac}(22 Hz) deviates from the $1/T$ law due to dynamical effects near T_m. Our χ_{ac} data are accurately fitted by a Curie law in a narrow range of T: $1.7T_m-3.2T_m$ with errors no larger than $2\times10^{-3}\chi$. We observed the same behavior in Ref. 12 for i-$Al_{73}Mn_{21}Si_6$. In the latter case we had the benefit of measurements of the magnetization in dc field for $H\rightarrow0$, and we noticed that the $1/T$ law applied down to $1.03T_m$. The C/T term is attributed to the magnetic Mn and χ_0 to nonmagnetic contributions. In a paramagnet or in a spin glass, $C=Nxp_{\text{eff}}^2/3k_B$, where N is the total number of atoms. In T-$Al_{80}Mn_{20}$ (T-$Al_{78}Mn_{22}$, respectively), we obtain a value of xp_{eff}^2, which is 27 (15, respectively) times smaller than that calculated if one assumes that all the Mn's carry a moment of $5\mu_B$. The same results occur in i phases and other T phases containing nearly the same amount of Mn.[13,14] However, we note that in the T phases, C is 2 to 3 times larger than in the i phases with similar concentration. Nevertheless, from the overall similarities of the magnetic behaviors between i and T phases, as will be described in the following, it is reasonable to assume that only a fraction of Mn sites are magnetic (as shown in Ref. 12 for the i phase) rather than having all Mn's carrying a moment of very low value. The contributions arising from the "nonmagnetic" Mn (Kondo-like) are then included in the χ_0 term of χ. In Table I we report values of x deduced by assuming $p_{\text{eff}}=5\mu_B$, since, at this step, we have no direct measurement of p_{eff} in these alloys.

Another way to deduce the number of magnetic Mn is provided by specific-heat (C_P) measurements performed down to very low T: 80 mK in our study. We present the C_P data in Fig. 6 for both T phases. The two T phases behave similarly: Above 0.5 K, the C_P data differ only by $\sim10\%$ and obey a quasilinear variation with temperature. Below 0.3 K, the rapid increase of C_P at decreasing T can be accurately fitted by

$$C_P=C_NT^{-2}+AT\ . \tag{1}$$

In the C_P-T diagram plotted on a double-logarithmic

TABLE I. Freezing temperature (T_m), temperature-independent susceptibility (χ_0), Curie constant (C), nuclear hyperfine term (C_N), linear term AT arising from the electronic γT term plus a magnetic term as deduced from the analysis of the specific-heat measurement (see text) for both decagonal T phases and amorphous (a) for comparison. x and x^* are the concentration of magnetic Mn atoms deduced from (C) and (C_N), respectively. Susceptibility data for a-$Al_{85}Mn_{15}$ extracted from Ref. 10.

	T_m (K)	χ_0 10^{-5} emu/g	C 10^{-4} emu/g	Fitting temp. range	A mJ/mol K^2	C_N 10^{-5} JK/mol	x 10^{-3}	x^* 10^{-3}
T-$Al_{80}Mn_{20}$	4.2±0.1	4.0±0.7	7.1±0.2	7K–12K	17	3.35±0.05	7	7.5
T-$Al_{78}Mn_{22}$	6.25±0.05	2.0±0.5	14±0.2	11K–20K	23	10±0.05	15	23
a-$Al_{85}Mn_{15}$	0.07	0.09	0.3	10K–70K	25	≤0.05		

scale inserted in Fig. 6, once a linear T term is subtracted to C_P, a T^{-2} term is observed over one decade of C_P. The values of A and C_N are reported in Table I. The T^{-2} term is the signature of a nuclear hyperfine magnetic contribution of the magnetic Mn's.[11] It is the case of transition metals (impurities) in a noble-metal matrix. Then the leader term in the magnetic hyperfine Hamiltonian is due to the core polarization interaction between the nuclear spin I of ^{55}Mn and the effective magnetic field H_{eff} induced by the electronic magnetization (spin S) of the *same atom*. Hence C_N is directly related to the concentration x^* of the moments close to their saturation value:[11]

$$C_N \alpha x^* |H_{\text{eff}}|^2 \sim x^* \langle S \rangle^2 . \quad (2)$$

Actually, other contributions to C_N exist, but they are of the second order in that case:[17] The first one comes from the dipolar interactions with magnetic Mn nearest neighbors in the case of small Mn clusters. The second one is due to electronic orbital interaction. The last contribution is induced by the magnetic Mn's on the nucleus of their Al nearest neighbors: In zero external field this contribution for one Al atom equals 1% of that of magnetic Mn.[18] So we assume that the ratio H_{eff}/S does not depend very much on the atoms surrounding one magnetic Mn and that it has the same value as in standard diluted Mn alloys such as *Cu*Mn or *Ag* Mn spin glasses. This

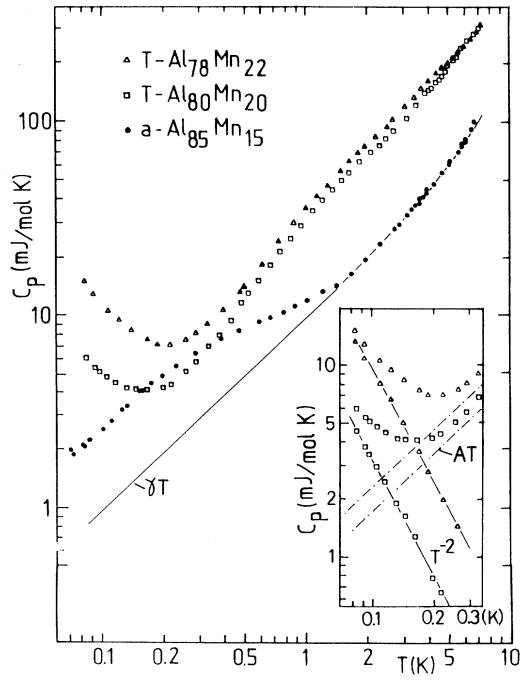

FIG. 6. Specific-heat data for T-$Al_{80}Mn_{20}$, T-$Al_{78}Mn_{22}$ and a-$Al_{85}Mn_{15}$. The continuous line represent the $\gamma T+\beta T^3$ analysis obtained for a-$Al_{85}Mn_{15}$. In the inset is shown the analysis of C_P below 0.3 K: $C_P = AT + C_N T^{-2}$ for the two decagonal phases. In a-$Al_{85}Mn_{15}$, the $C_N T^{-2}$ term would exist, but well below 80 mK.

has two main consequences. First we can take for H_{eff} a value of 27 ± 2.5 T as in CuMn or AgMn, if we assume the same value of the spin in CuMn, and the QC phases. The second consequence is that x^* should equal the concentration of magnetic Mn atoms. In contrast, in Ref. 12 what we deduced was the number of magnetic entities that can be very small clusters of highly correlated magnetic Mn. Taking the same previous H_{eff} value yields $x_p^*=7.5\times10^{-3}$ and 23×10^{-3} for the two T phases (see Table I). In comparison, we found previously[11] that $x^*=8.5\times10^{-3}$ (i.e., 4% of the total Mn's) in i-$Al_{75}Mn_{20}Si_5$.

In conclusion, we deduce values of x and x^* very close for a same sample once we assume a moment equal to $5\mu_B$ in the Curie constant. These values are much lower than the nominal concentration of Mn and increase rapidly (by a factor 2 or 3) when the amount of Mn is only increased from 20 to 22 at. %.

IV. ORIGIN OF THE MAGNETIC INTERACTIONS BETWEEN MAGNETIC MOMENTS

Since a very few Mn's are magnetic, each is far from the others, and one can expect only indirect long-range exchange interactions between them, i.e., RKKY interactions of intensity $J_{ij}\alpha V_0/r_{ij}^3$. Then T_m, obtained from χ_{ac} measured at the same frequency for various spin concentrations, is a temperature characteristic of the interaction and should scale as

$$\langle J_{ij}S_iS_j\rangle = V_0S(S+1)/r^3 .$$

Here r is the mean distance between the spins and V_0 depends on the band structure. As $1/r^3\sim x$, one finds $\langle J_{ij}\rangle\sim V_0x$ and $T_m\sim Nxp_{\text{eff}}^2$. Actually, a more careful analysis[19] in standard RKKY spin glasses shows deviations to an exact linear law of T_m versus x explained by self-damping effects[20] of the long-range J_{RKKY}, which develops at large concentrations ($x>$ a few 10^{-3}): One finds $T_m=T_0x^{0.7}$ (for CuMn and AuMn in Ref. 19), where T_0 depends on V_0, i.e., on the system.

Here we confirm our previous statement: In all the Al-Mn QC and a phases, the magnetic correlations are due to RKKY interactions. We also show that V_0 does not depend on the structure (a, i, or T). First we find that T_m increases as the Curie constant, i.e., as Nxp_{eff}^2 in our T phases (see Table I). Secondly when we plot T_m versus the hyperfine specific heat C_N (i.e., x^*) in a log-log diagram together with previous data obtained in i and a phases[10,11] (see Fig. 7), we observe that all the data align on a *single* straight line of slope 0.8 over 2 decades up to 6 K: $T_m=T_0C_N^{0.8}$, T_0 and therefore V_0 being the same for all Al-Mn QC and a phases.

Another evidence for RKKY interactions is given by the dependence of C_m on the concentration of the magnetic Mn's: $C_m(T)$ is the standard magnetic part of the specific heat involved in the AT term of Eq. (1): $AT=\gamma T+C_m(T)$, where γT is the electronic term. C_m is proportional to the number of spins (Nx) times a function of $T/\langle J_{ij}\rangle$. For C_m linear with T ($C_m=BT$), $B\sim x/\langle J_{ij}\rangle$ is then independent of x for RKKY interactions. Before a quantitative analysis of A, we observe that the quasilinear terms ($\sim T^{1.1}-T^{1.2}$) of the C_P data above 0.5 K are similar for the two T phases, and when extrapolated down to 0.1 K, also similar to the a-$Al_{85}Mn_{15}$ data (shown also in Fig. 6). This indicates an almost independence of A on the magnetic Mn concentration. Indeed, the number of magnetic Mn is at least 50 times smaller in a-$Al_{85}Mn_{15}$ than in our T phases (see Fig. 7). From the fit (1) for our T phases, we deduce that in the temperature range (0.08–0.3 K) $C_m(T)$ is linear with T: $C_m(T)=BT$. To deduce $C_m(T)$, i.e., B, implies to know γ and therefore needs an analysis well above T_m, where $C_m(T)$ vanishes. Since T_m is large for our T phases, we should measure C_P at high temperatures, i.e., in a range where the phonon contribution is large and can make the determination of γ difficult. This prevents an accurate determination of B in this case. We do not have this problem in a-$Al_{85}Mn_{15}$:[21] T_m is very small (70 mK), and $C_m(T)$ vanishes at 2 K (see Fig. 7) above which the γT term can be deduced accurately ($\gamma=9.5$ mJ/mol K^2 and $B=15$ mJ/mol K^2). We found a similar result[21] for the a phase of other compositions $Al_{82.7}Mn_{17.3}$ ($\gamma=11.7\pm0.3$ mJ/mol K^2 and $B=8$ mJ/mol K^2) for which $T_m=0.65$ K. In both cases, B is of the order of magnitude of γ although T_m varies by one order of magnitude. So we can present the following conclusions. Since A is nearly a constant (see Table I), if we assume that γ does not vary too much within this limited Mn concentration range (15–22 at. %), we deduce for a and T phases a general agreement with B being nearly (within a factor 2) independent of the magnetic Mn concentration x^* over a wide range *(two orders of magnitude)* of x^*. The quasi-independence of $C_m(T)$ on the concentration of spins is the signature of RKKY interactions early checked experimentally in canonical metallic spin glasses.[22]

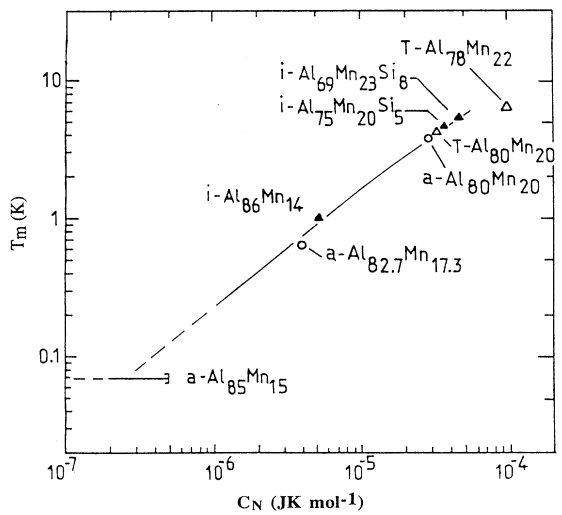

FIG. 7. Freezing temperature as measured by χ_{ac} at 115 Hz (or 22 Hz for T-$Al_{78}Mn_{22}$) vs the amplitude of the nuclear hyperfine term in C_P for all the amorphous and quasicrystalline (icosahedral and decagonal T samples).

Finally for the two T phases, we note that in the temperature range 0.3–7 K $C_m(T)$ varies roughly as $T^{1.2}-T^{1.4}$ once we have subtracted a γT term of about 10 mJ/mol K. Such deviations to an exact linearity are also reported in metallic spin glasses, such as Cu-Mn, generally below 1 K.[23,24] In icosahedral phases, we previously observed even more rapid variations for $C_m(T)$. Smooth bumps centered around $T=1$ K also appears as a common characteristic of the QC phases we measured[10] (i-$Al_{86}Mn_{14}$ and i-$Al_{75}Mn_{20}Si_5$) and also of i-$Al_{80}Mn_{20}$ and T-$Al_{78}Mn_{22}$ as reported elsewhere.[14]

In conclusion, we have shown that both T_m and C_P scale with the concentration of really magnetic Mn's following the predictions specific to RKKY interactions. The same scalling, involving the same prefactors, is obeyed for all the a, i and T phases, indicating that the RKKY potential is independent on the structure (a, i, or T). Thus we can conclude that the correlations between spins can extend over large distances at low T[12]. At high T's, the correlations can only persist between nearest neighbors. The appearance of a Curie-Weiss temperature Θ in χ_{ac} above $3.2T_m$ (see Sec. III) is directly related to the amplitude and the sign of these nearest-neighbor interactions.

V. EVIDENCE OF AN ANOMALOUS HALL EFFECT, RELATION TO THE MAGNETIZATION

We present here the first Hall effect measurement of pure T-$Al_{80}Mn_{20}$ and T-$Al_{78}Mn_{22}$ phases with respect to its correlation with the measured magnetization. In Fig. 8, the total Hall resistivity ρ_H, measured at fixed temperatures from 0.5 to 110 K, is plotted versus the dc applied field ($H=0$ to 8 T). The Hall coefficient defined by $R_H=\rho_H/H$ is always positive. The curves $\rho_H(H)$ look like standard magnetization curves. Indeed ρ_H is linear in H up to 8 T at high T, while strong curvatures appear at low field and low T. In addition the initial slope in the zero-field limit varies essentially as $1/T$ above 6 K. Similar behaviors were observed in i-Al-Mn phases.[25]

The existence of an anomalous Hall effect, i.e., that saturates at high field and depends on temperature, is typical of metals with local moments. In this case, the Hall resistivity ρ_H is analyzed as the sum of two main effects: The classical Hall effect due to the Lorentz force acting on the carriers and the anomalous Hall effect ascribed to an anisotropic scattering of the conduction electrons by local moments.[26] ρ_H is then written with the phenomenological relation (in cgs units): $\rho_H=R_0B+R_S4\pi M$, with B the magnetic induction, M the macroscopic intensity of magnetization, and R_0 and R_S the ordinary and anomalous Hall coefficients, respectively. Then,

$$\rho_H=R_0H+[4\pi R_S+R_0(4\pi-N)]M \ ,$$

where H is the applied magnetic field and N is the depolarization factor. This expression becomes

$$\rho_H=R_0H+4\pi R_SM \ , \tag{3}$$

since in the usual geometry of the magnetic field perpendicular to a flat slab sample $N\approx 4\pi$,[27] and $|R_S| \gg |R_0|$ as it is seen later on.

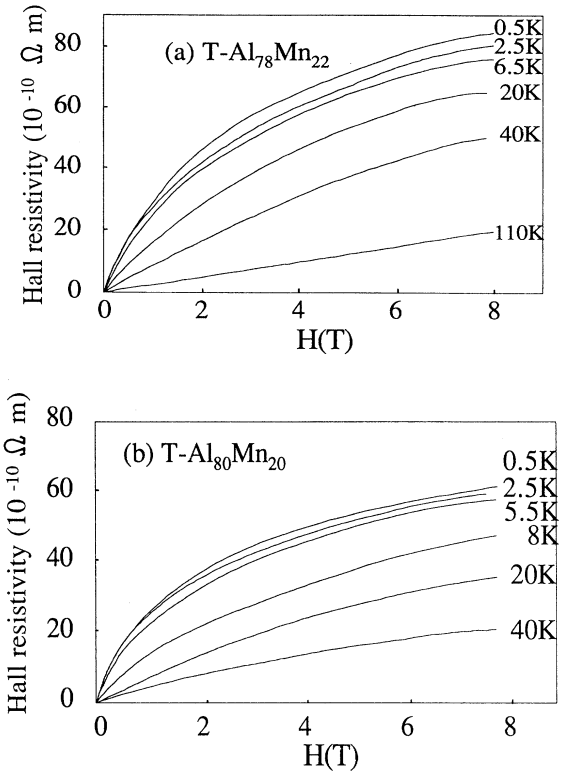

FIG. 8. Hall resistivity vs magnetic field (0–8 T) at different temperature in T-$Al_{78}Mn_{22}$ and T-$Al_{80}Mn_{20}$.

Our goal is to correlate directly ρ_H to M, which we measured on the same sample (T-$Al_{78}Mn_{22}$), at the same dc fields and temperatures. At constant temperature (6.5, 20, and 40 K), ρ_H/H is linear with M/H, as can be seen in Fig. 9. This proves the validity of Eq. (3) over our range of H: 0-7 T. Since all the data obtained at 20 and 40 K are aligned on the same straight line, we deduce that R_0 and R_S ($=4.7\pm0.1\times10^{-7}$ m^3/C for T-$Al_{78}Mn_{22}$) are T independent in this temperature range. The slightly different value of R_S (4.5×10^{-7} m^3/C) found at 6.5 K (see Fig. 9) may indicate a small dependence of R_S on T when the system is close to the low-temperature spin-glass phase. But also, it can be not relevant due to the different cryostats used in the two measurements of ρ_H and M with different problems of temperature control at low temperature. To extend our study over a wide range of temperature, we have also correlated M to ρ_H at low fields ($H<0.4$ T). Above 16 K, ρ_H and M are linear in H: The initial slopes $d\rho_H/dH$ and dM/dH can be easily deduced, since they are equal to ρ_H/H and M/H, respectively, for any field up to 0.4 T. In the same range of temperature, dM/dH (with H being static) is also equal to χ_{ac}, since no frequency effects in χ_{ac} are observed at high T's (at least for low frequencies). Below 16 K, the strong curvatures of $M(H)$, which appear at low fields are due to the increase of the nonlinear field terms of M at decreasing T.[12] The same cur-

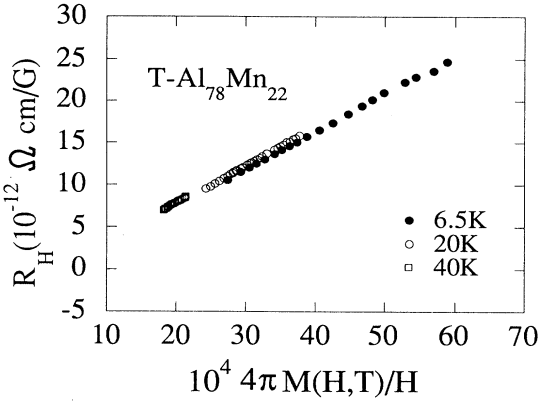

FIG. 9. Linear dependence of ρ_H/H upon $M(H,T)/H$ with H varying from 0 to 7 T and at different temperatures.

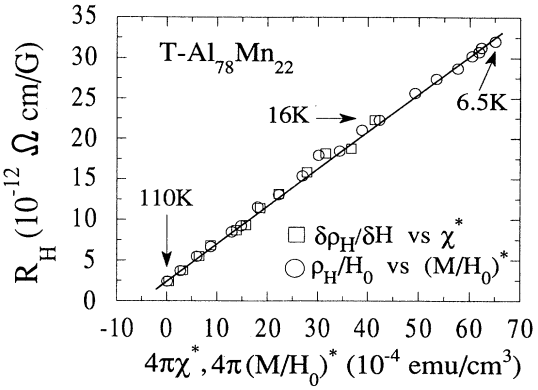

FIG. 10. Linear dependence of ρ_H/H_0 upon the effective magnetic susceptibility (M/H_0^*) at $H_0=0.39$ T and $\delta\rho_H/\delta H$ vs χ^* for T-$Al_{78}Mn_{22}$. $\chi^*=\chi(T)-\chi_0$ and $(M/H_0)^*=M/H_0-\chi_0$.

vatures are observed in $\rho_H(H)$. This makes it difficult to deduce very accurate values of the initial slopes $d\rho_H/dH$ and dM/dH at low T, since they should be obtained at very low field (below 10^{-3} T), i.e., where ρ_H and M are very small. So we choose to compare ρ_H/H and M/H measured in a moderate field $H_0=0.39$ T, where ρ_H and M are large enough to be estimated accurately in our experimental setup. We summarize our results for T-$Al_{78}Mn_{22}$ in Fig. 10, where we plot ρ_H/H_0 versus M/H_0 in the whole temperature range and $d\rho_H/dH$ versus dM/dH and versus χ_{ac} above 16 K.

For a given Mn concentration, all the data are aligned on a single straight line in Fig. 10. In this plot we have subtracted the value of χ_0 to M/H (and to dM/dH and χ_{ac}), since M in Eq. (3) is the magnetization due to the magnetic moments only. We conclude that our data are accurately fitted by Eq. (3), and we can deduce R_S. For both T phases, R_S is positive. We find $R_S=3.2\pm0.3\times10^{-7}$ m^3/C and $4.8\pm0.2\times10^{-7}$ m^3/C for T-$Al_{80}Mn_{20}$ and T-$Al_{78}Mn_{22}$, respectively (see Table II). An accurate determination of R_0 is very difficult because it depends strongly on the accuracy on the χ_0 term. We can only note that the anomalous Hall coefficient R_S is by at least a factor 10^4 larger than R_0, which means that the anomalous contribution dominates considerably that arising from the Lorentz force. Generally, the density n of carriers is deduced from R_0. As we have $|R_0|<10^{-10}$ m^3/C, which correspond to the maximum error made in the determination of χ_0, we have $n>10^{23}$/ cm^3. Anyway, as no band-structure effect is taken into account, one should remain very careful about the physical meaning of n in these complex systems.

The measured positive Hall coefficient R_H is thus due to the anomalous Hall effect, arising from the presence of magnetic moments.[28,29] This contribution, observed in a variety of systems such crystalline rare-earth phases,[26] paramagnetic or ferromagnetic amorphous alloys,[30] and canonical spin glasses,[31,32] is attributed to spin-orbit couplings that can give rise to skew scattering and/or to side jump mechanisms.[33] The first mechanism appears when there is a difference between the probabilities of scattering to the left and right of the polarization direction of the localized moment. The nonclassical side jump mechanism has been initially developed for ferromagnetic systems and results also from spin-orbit interaction and leads to a displacement of the center of mass of the electron's wave packet. The anomalous Hall effect is thought to be dominated by skew scattering in dilute alloys[34] (having small ρ), and by the side jump mechanism in amorphous or disordered alloys having short mean free paths.[26]

Al-Mn T-phases exhibit the magnetic behavior of spin glasses with a small concentration of spins. But R_S is of opposite sign and one order of magnitude larger than that measured in the spin glasses, which exhibit a strong spin-orbit coupling (AuMn and AuFe). Moreover, it was not at all expected to find such a high value in an Al-Mn alloy, for which neither Al nor Mn are known to possess strong spin-orbit coupling when diluted in a crystalline matrix (Cu and Ag, for instance). However, a similar value of R_S (8.1×10^{-7} m^3/C) has been measured in the

TABLE II. Resistivity values at 0.3 K ($\rho_{0.3\,K}$) and at 300 K ($\rho_{300\,K}$), temperature coefficient of resistiviy, at 300 K ($\alpha_{300\,K}$) R_S is the anomalous Hall coefficient deduced from the analysis of Hall effect and magnetization measurements for decagonal samples T-$Al_{78}Mn_{22}$ and T-$Al_{80}Mn_{20}$.

	$\rho_{0.3K}$ ($\mu\Omega$ cm)	$\rho_{300\,K}$ ($\mu\Omega$ cm)	$\alpha_{300\,K}$ (10^{-4} K^{-1})	R_S 10^{-7} m^3/C
T-$Al_{80}Mn_{20}$	430±20	420±20	−1.8	3.2±0.4
T-$Al_{78}Mn_{22}$	480±30	430±20	−3	4.8±0.2

high-temperature paramagnetic region of an Al-Mn phase but very different from our T phases: It is a crystalline ordered alloy[35] ($Al_{0.89}Mn_{1.11}$), which is a ferromagnet below $T_c = 679$ K. Now, comparing with other systems, we find the R_S is of the same sign and magnitude as the amorphous alloy highly concentrated in spins $Zr_{65}Fe_{35}$ (Ref. 36), which is a paramagnet ($R_S = 4.3 \pm 0.1 \times 10^{-7}$ m^3/C). In the latter case, R_S has been attributed to side jump effect. We finally comment on the sign of R_S. These spin-orbit contributions (side jump effect or skew scattering) depend on the band structure. For instance, for ferromagnets the sign of R_S is predicted and observed to change depending on the location of the Fermi level in these bands.[26] But in our case, the band structure is not known up to now, which prevents any prediction about the sign of R_S.

VI. MAGNETORESISTANCE

Another way to investigate the scattering of electrons by magnetic moments is to measure the magnetoresistance (MR). the MR $\Delta\rho/\rho$ is plotted as a function of magnetic field H (up to 8 T) at different temperatures (0.3–60 K) in Fig. 11. For both samples, no difference was observed between the longitudinal and transverse MR (within our accuracy). At the lowest temperature (0.3 K), the MR for both alloys in negative. T-$Al_{78}Mn_{22}$ presents stronger negative MR than T-$Al_{80}Mn_{20}$ and keeps negative contributions at higher temperatures. We also note that at low temperature the MR increases with temperature (from negative to positive values), while it decreases and vanishes at higher temperature (see the insert of Fig. 11).

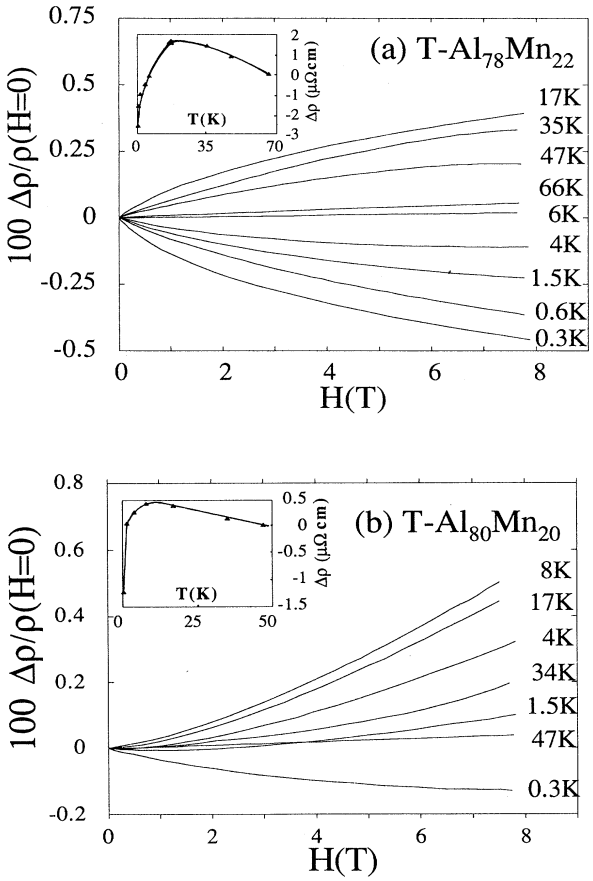

FIG. 11. Longitudinal magnetoresistance measurement in T-$Al_{78}Mn_{22}$ and T-$Al_{80}Mn_{20}$. In the inset is shown $\Delta\rho = \rho(H = 7T) - \rho(H = 0)$ vs T.

The measured MR results from competing positive and negative contributions. First of all, we can neglect the positive *normal* MR $\Delta\rho/\rho_{\text{normal}}$ due to the Lorentz force. Indeed, at high temperature ($T > 70$ K), the MR vanishes for both samples, and also we estimate $\Delta\rho/\rho_{\text{normal}} < 10^{-10}$, which is 10^7 times lower than our data. Here

$$\Delta\rho/\rho_{\text{normal}} = (1/ne)^2 (H/\rho)^2 ,$$

with n being the density of carriers that we deduce from the Hall effect measurements ($n > 10^{23}$ cm^3). A positive MR has been reported in some amorphous magnetic alloys[37,38] and interpreted in terms of magnetic origin. Due to the difficulties to know accurately the small variation of ρ with field ($\Delta\rho/\rho < 10^{-2}$ in 8 T), we did not succeed in quantitatively correlating the magnetization and MR data.

The negative part of the MR may be associated with magnetic contributions. The negative contribution of the MR observed at low temperature for both T phases is similar to that measured in canonical spin glasses for which the MR is found to be negative at all temperatures (1.5–77 K) and fields.[39] Moreover, as in our case, the magnitude $|\Delta\rho/\rho|$ increases with field and decreases with temperature, and $|\Delta\rho|$ increases with impurity (Mn) concentration. Based on an Edwards-Anderson-type model, Mookerjee[40] calculated the MR in spin glasses, and most of the characteristic features of the canonical spin glasses have been qualitatively explained.

CONCLUSION

In summary, the measured magnetic susceptibility, specific-heat, and transport properties of the pure Al-Mn T-phase $Al_{80}Mn_{20}$ and $Al_{78}Mn_{22}$ are consistent with the presence a low fraction of magnetic Mn sites that increase with the Mn concentration and interact through RKKY interaction. These behaviors are very similar to that of the corresponding icosahedral and amorphous phases but in striking difference with the crystalline phases of the same composition, which show no moment. The origin of local magnetic moments in QC phases is still unanswered, but it may be due to Mn clusters as proposed in Ref. 12.

The Hall coefficient $R_H = \rho_H/H$ of both decagonal phases is linear with M/H. This anomalous Hall contribution is unexpectedly strong. The order of magnitude of the linear coefficient R_S is comparable to that of amorphous paramagnetic Zr-Fe highly concentrated in spins, while our T phases contain a small number of moments. This value can be associated with a strong spin-orbit scattering unexpected in such alloys.

ACKNOWLEDGMENTS

We acknowledge fruitful discussions with F. Cyrot Lackmann, T. Klein, and D. Mayou. We also wish to thank J. C. Grieco for preparing the samples, I. Levi (Technion Haifa-Israel) for Transmission electron microscopy (TEM) examinations, and M. Godinho for preliminary susceptibility measurement.

[1]L. Bendersky, Phys. Rev. Lett. **55**, 1461 (1985).
[2]D. Shechtman, I. Blech, D. Gratias, and J. W. Cahn, Phys. Rev. Lett. **53**, 1951 (1984).
[3]P. Guyot and M. Audier, J. Microsc. Spectrosc. Electron. **10**, 575 (1985).
[4]J. M. Dubois, C. Janot, J. Pannetier, and A. Pianelli, Phys. Lett. A **117**, 421 (1986).
[5]F. Bridges, J. B. Boyce, G. M. Dimino, and B. C. Giessen, Phys. Rev. B **36**, 8973 (1987); P. J. Schurer, T. J. Van Netten, and L. Niesen, J. Phys. (Paris) **49**, 237 (1988); A. Sadoc, A. M. Flank, P. Lagarde, and J. M. Dubois, Int. J. Mod. Phys. B **1**, 133 (1987).
[6]S. Takeuchi and K. Kimura, J. Phys. Soc. Jpn, **56**, 982 (1987); V. Kumar, D. Sahoo, and G. Athithan, Phys. Rev. B **34**, 6924 (1986).
[7]A. P. Tsai, A. Inoue, and T. Masumoto, Mater. Trans. JIM **30**, 300 (1989).
[8]A. Gozlan *et al.* (unpublished).
[9]C. Berger, A. Gozlan, G. Fourcaudot, F. Cyrot Lackmann, 10th G^{al} Conference on Condensed Matter. EPS (Lisbon, 1990) [Phys. Scr. T **35**, 90 (1991)].
[10]C. Berger, J. C. Lasjaunias, J. L. Tholence, D. Pavuna, and P. Germi, Phys Rev. B **37**, 6525 (1988); C. Berger, K. Hasselbach, J. C. Lasjaunias, C. Paulsen, and P. Germi, J. Less Common Met. **145**, 565 (1988).
[11]J. C. Lasjaunias, J. L. Tholence, C. Berger, and D. Pavuna, Solid State Commun. **64**, 425 (1987); J. C. Lasjaunias, M. Godhino, and C. Berger, Physica B **165-166**, 187 (1990).
[12]C. Berger and J. J. Prejean, Phys. Rev. Lett. **64**, 1769 (1990).
[13]F. Hippert, P. Monod, R. Bellissent, and F. Vigneron, J. Phys. (Paris) **49**, C8-235 (1988).
[14]F. L. A. Machado, W. G. Clark, D. P. Yang, W. A. Hines, L. J. Azevedo, B. C. Giessen, and M. X. Quan, Solid State Commun. **61**, 691 (1987); F. L. A. Machado, W. W. Kang, P. C. Canfield, W. G. Clark, B. C. Giessen, and M. X. Quan, Phys. Rev. B **38**, 8088 (1988).
[15]A. Gozlan, C. Berger, G. Fourcaudot, J. C. Grieco, F. Cyrot-Lackmann, and P. Germi, Solid State Commun. **75**, 417 (1990).
[16]W. W. Warren, H.-S. Chen, and G. P. Espinosa, Phys. Rev. B **34**, 4902 (1986).
[17]See, e.g., *Hyperfine Interactions,* edited by A. J. Freeman and R. C. Frankel, (Academic, New York, 1967).
[18]B. Caroli, and A. Blandin, J. Phys. Chem. Solids, **27**, 503 (1966).
[19]V. Cannella, in *Amorphous Magnetism I* edited by H. O. Hooper and M. de Graaf (Plenum, New York 1973), p. 195.
[20]U. Larsen, Solid State Commun. **22**, 311 (1987).
[21]M. Godinho, C. Berger, J. C. Lasjaunias, K. Hasselbach, and O. Bethoux, J. Non-Cryst. Solids **117-118**, 808 (1990).
[22]J. Souletie and R. Tournier, J. Low Temp. Phys. **1**, 95 (1969).
[23]L. E. Wenger and P. H. Keesom, Phys. Rev. B **13**, 4053 (1976); D. L. Martin, Phys. Rev. B **20**, 368 (1980); **21**, 1902 (1980).
[24]W. H. Fogle, J. C. Ho, and N. E. Phillips, J. Phys. (Paris) **39**, C6-901 (1978); R. Caudron, P. Costa, J. C. Lasjaunias, and B. Levesque, J. Phys. F **11**, 451 (1981).
[25]O. Laborde, J. M Frigerio, J. Rivory, A Perez, and J. C. Plenet, Solid State Commun. **71**, 711 (1989).
[26]C. M. Hurd, *The Hall effect in Metals and Alloys* (Plenum, New York, 1972).
[27]R. I. Joseph and E. Schlomann, J. Appl. Phys. **36**, 1579 (1965).
[28]L. Berger and G. Bergmann, in *The Hall Effect and Its Applications,* edited by C. L. Chien and C. R. Westgate (Plenum, New York, 1980), p. 55.
[29]A. Fert and A. Hamzic, in *The Hall Effect and Its Applications* (Ref. 28), p. 77.
[30]R. C. O'Handley, Phys. Rev. B **18**, 2577 (1978).
[31]R. D. Barnard and I Ul-Haq, J. Phys. F **18**, 1253 (1988).
[32]S. P. McAlister and C. M. Hurd, Solid State Commun. **19**, 881 (1976); J. Phys. F **8**, 239 (1978).
[33]C. M. Hurd, Contemp. Phys. **16**, 517 (1975).
[34]A. Fert, A. Friederich, and A. Hamzic, J. Magn. Magn. Mater. **24**, 231 (1981).
[35]B. Babic, M. Stojic, J. Konstantinovic, M. Napijalo, and L. Novakovic, J. Phys. F **14**, 3015 (1984).
[36]M. Trudeau, R. W. Cochrane, D. V. Baxter, J. O. Strom-Olsen, and W. B. Muir, Phys. Rev. B **37**, 4499 (1988).
[37]Y. Z. Wang, F. M. Yang, Y. S. Wu, M. Y. Feng, and W. S. Zhan, J. Magn. Magn. Mater. **31-34**, 1473 (1983).
[38]R. R. Hake, M. G. Karkut, and S. Aryainejad, Solid State Commun. **35**, 709 (1980).
[39]A. Nigam and A. K. Majumdar, Phys. Rev. B **27**, 495 (1983).
[40]A. Mookerjee, J. Phys. F **10**, 1559 (1980).

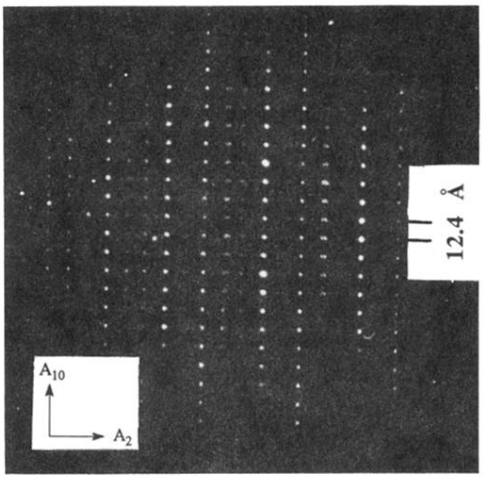

FIG. 2. Electron diffraction pattern taken along a twofold zone axis for decagonal T-$Al_{78}Mn_{22}$ phase.

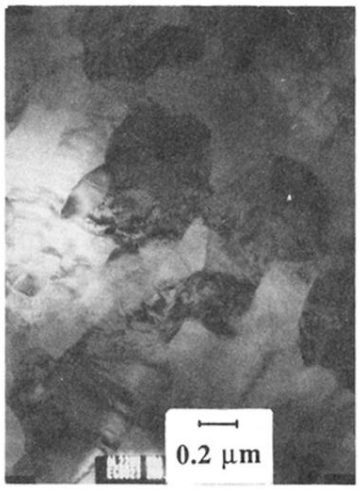

FIG. 3. Microstructure of decagonal T-$Al_{78}Mn_{22}$ phase observed by transmission electron microscopy.